

# Closed orbits and their bifurcations in the crossed-fields hydrogen atom

Thomas Bartsch, Jörg Main, and Günter Wunner

*Institut für Theoretische Physik 1, Universität Stuttgart, D-70550 Stuttgart, Germany*

(Dated: October 29, 2018)

A systematic study of closed classical orbits of the hydrogen atom in crossed electric and magnetic fields is presented. We develop a local bifurcation theory for closed orbits which is analogous to the well-known bifurcation theory for periodic orbits and allows identifying the generic closed-orbit bifurcations of codimension one. Several bifurcation scenarios are described in detail. They are shown to have as their constituents the generic codimension-one bifurcations, which combine into a rich variety of complicated scenarios. We propose heuristic criteria for a classification of closed orbits that can serve to systematize the complex set of orbits.

PACS numbers: 32.60.+i, 32.80.-t, 03.65.Sq, 05.45.-a

## I. INTRODUCTION

Closed-orbit theory [1, 2] has proven to be the key tool to analyze the photoabsorption spectra of atoms in external fields. It interprets spectral oscillations semiclassically in terms of closed orbits of the underlying classical system, i.e. of classical orbits starting at and returning to the nucleus. A complete semiclassical description of an atomic spectrum therefore requires a sufficiently detailed understanding of the classical closed orbits. In particular, the possible types of closed-orbit bifurcations must be described, so that the generation of new closed orbits upon varying the external field strengths can be accounted for.

For the hydrogen atom in a magnetic field, the systematics of closed orbits and their bifurcations has been known for a long time [3, 4, 5, 6, 7, 8]. For the hydrogen atom in crossed electric and magnetic fields, the classical mechanics is much more complicated because three non-separable degrees of freedom have to be dealt with. Although a number of closed orbits have been identified in experimental or theoretical quantum spectra [3, 9, 10, 11, 12], a systematic study of these orbits and their bifurcations is still lacking.

Considerable effort has been spent during the past decade on the study of the classical mechanics of the crossed-fields hydrogen atom in the limit of weak external fields [13, 14, 15, 16, 17]. That work relies on the observation that for weak external fields the principal quantum number  $n$ , or its classical analogue  $n = 1/\sqrt{-2E}$ , is conserved to a higher degree of precision than the angular momentum and Lenz vectors  $\mathbf{L}$  and  $\mathbf{A}$ . The latter are conserved in the pure Kepler problem, but acquire a slow time-dependence in weak fields, so that the electron can be visualized as moving on a slowly precessing Kepler ellipse.

The most important result in the present context is the finding first described in [14] that there are four Kepler ellipses that remain unperturbed by the external fields to first order in the field strength, i.e. among the continuous infinity of periodic orbits of the unperturbed Kepler problem there are four orbits that are periodic even in the presence of external fields. These fundamental peri-

odic orbits can be regarded as the roots of “family trees” of periodic orbits. More complicated orbits are created out of the fundamental orbits by bifurcations as the field strengths increase.

However, none of the fundamental periodic orbits is closed at the nucleus. Their knowledge therefore does not aid in the classification of closed orbits. A first systematic study of closed orbits in the crossed-fields system and their bifurcations was performed by Wang and Delos [18]. These authors presented orderly sequences of bifurcations of planar closed orbits (i.e. orbits in the plane perpendicular to the magnetic field), which they interpreted in terms of an integrable model Hamiltonian.

In the present paper we undertake a systematic investigation of closed orbits and their bifurcations in the crossed-fields hydrogen atom. In section II, the symmetries of the Hamiltonian are briefly reviewed. Section III A presents the general framework of a local bifurcation theory of closed orbits, and section III B describes the generic codimension-one bifurcations. A discussion of complex ghost orbits is included in each case because they are known to play an important role in semiclassics [19, 20]. In section IV, the closed orbits in the hydrogen atom in a magnetic field are surveyed. Section V then details the bifurcation scenarios actually observed in the crossed-fields system. It is shown that the elementary codimension-one bifurcations actually form the building blocks of the bifurcations scenarios, but that in many cases complicated scenarios consisting of several elementary bifurcations occur. In section VI, a heuristic classification scheme for the closed orbits in crossed fields is proposed which is based on the well-known classification for the closed orbits in a magnetic field. The actual semiclassical quantization of the crossed-fields hydrogen atom in the framework of closed-orbit theory, which is based on the results presented here, is described in an accompanying paper [21].

## II. THE CLASSICAL HAMILTONIAN

Throughout this work, we will assume the magnetic field to be directed along the  $z$ -axis and the electric field

	Transformation				Symmetry conditions
	$\vartheta_i$	$\varphi_i$	$\vartheta_f$	$\varphi_f$	
Z	$\pi - \vartheta_i$	$\varphi_i$	$\pi - \vartheta_f$	$\varphi_f$	$\vartheta_i = \vartheta_f = \frac{\pi}{2}$
T	$\vartheta_f$	$-\varphi_f$	$\vartheta_i$	$-\varphi_i$	$\vartheta_i = \vartheta_f$ and $\varphi_i = -\varphi_f$
C	$\pi - \vartheta_f$	$-\varphi_f$	$\pi - \vartheta_i$	$-\varphi_i$	$\vartheta_i = \pi - \vartheta_f$ and $\varphi_i = -\varphi_f$

TABLE I: The symmetry transformations of the crossed-fields system: Transformation of initial and final angles and symmetry conditions for doublets. Singlets satisfy  $\vartheta_i = \vartheta_f = \frac{\pi}{2}$  and  $\varphi_i = -\varphi_f$ .

to be directed along the  $x$ -axis. In atomic units, the Hamiltonian describing the motion of the atomic electron then reads

$$H = \frac{1}{2}\mathbf{p}^2 - \frac{1}{r} + \frac{1}{2}BL_z + \frac{1}{8}B^2\rho^2 + Fx, \quad (1)$$

where  $r^2 = x^2 + y^2 + z^2$ ,  $\rho^2 = x^2 + y^2$  and  $L_z$  is the  $z$ -component of the angular momentum vector. By virtue of the scaling properties of the Hamiltonian (1), the dynamics does not depend on the energy  $E$  and the field strengths  $B$  and  $F$  separately, but only on the scaled energy  $\tilde{E} = B^{-2/3}E$  and the scaled electric field strength  $\tilde{F} = B^{-4/3}F$ . Upon scaling, all classical quantities are multiplied by suitable powers of the magnetic field strength  $B$ . In particular, classical actions scale according to  $\tilde{S} = B^{-1/3}S$ . These scaling prescriptions will be used throughout this work.

In crossed fields, two angles are required to characterize the starting or returning direction of a closed orbit. We will use the polar angle  $\vartheta$  between the trajectory and the magnetic field axis and the azimuthal angle  $\varphi$  between the projection of the trajectory into the  $x$ - $y$ -plane and the electric field axis.

The hydrogen atom in crossed fields does not possess any continuous symmetries so that, apart from the energy, no constant of the motion exists and three non-separable degrees of freedom have to be dealt with. There are, however, three discrete symmetry transformations of the crossed-fields system, namely

- the reflection Z at the  $x$ - $y$ -plane,
- the combination T of time-reversal and a reflection at the  $x$ - $z$ -plane,
- the combination C=ZT of the above.

The effects of the transformations on the initial and final angles of a closed orbit are summarized in table I.

The application of these transformations to a given closed orbit yields a group of four closed orbits of equal length. Typically, these orbits will all be distinct, so that closed orbits in the crossed-fields system occur in quartets. In particular cases, a closed orbit can be invariant under one of the symmetry transformations. In this case, there are only two distinct orbits related by symmetry transformations. We will refer to them as a doublet,

or more specifically as a Z-, T-, or C-doublet, giving the transformation under which the orbits are invariant. The transformations of the initial and final angles listed in table I yield symmetry conditions that an orbit invariant under any of the transformations must satisfy. These are also given in table I. In special cases, a closed orbit can be invariant under all three symmetry transformations. It then occurs as a singlet, since no distinct orbits can be generated from it by a symmetry transformation.

Among the symmetry transformations, the reflection Z plays a special role in that it is a purely geometric transformation. There is, therefore, an invariant subspace of the phase space, viz. the  $x$ - $y$ -plane perpendicular to the magnetic field. This plane is invariant under the dynamics and therefore forms a subsystem with two degrees of freedom.

In connection with bifurcations of orbits it is essential for semiclassical applications to study complex “ghost” orbits along with the real orbits, i.e. to allow coordinates and momenta to assume complex values. For ghost orbits, another reflection symmetry arises, viz. the symmetry with respect to complex conjugation. Since the Hamiltonian (1) is real, it is invariant under complex conjugation. Therefore, ghost orbits always occur in pairs of conjugate orbits.

### III. CLOSED-ORBIT BIFURCATION THEORY

#### A. General theory

The dynamics of the hydrogen atom in a pure magnetic field possesses time-reversal invariance if it is restricted to the subspace of vanishing angular momentum  $L_z$ . Due to this symmetry, an electron returning to the nucleus will rebound from the Coulomb center into its direction of incidence and retrace its previous trajectory back to its starting direction. Therefore, any closed orbit is either itself periodic or it is one half of a periodic orbit. Due to the close link between closed orbits and periodic orbits, closed-orbit bifurcations can be described in the framework of periodic-orbit bifurcation theory developed by Mayer [8, 22]. In particular, in a magnetic field closed orbits possess repetitions, so that arbitrary  $m$ -tupling bifurcations are possible.

In the presence of crossed electric and magnetic fields, the time-reversal invariance is broken, and no general connection between closed orbits and periodic orbits remains. As a consequence, the techniques of periodic-orbit bifurcation theory are no longer applicable, and a novel approach to the classification of closed-orbit bifurcations must be found. In this section, a general framework for the discussion of closed-orbit bifurcations will be introduced.

The crucial step in the development of the bifurcation theory of periodic orbits is the introduction of a Poincaré surface of section map in the neighborhood of the orbit. The Poincaré map describes the dynamics of the degrees

of freedom transverse to the orbit, and the orbit bifurcates when the transverse dynamics becomes resonant with the motion along the orbit.

For periodic orbits, a Poincaré map is specified by fixing a surface of section in phase space which is transverse to the orbit. For a point  $P$  on the surface of section, the trajectory starting at  $P$  is followed until it intersects the surface of section again. This intersection point is defined to be the image of  $P$  under the Poincaré map. The periodic orbit itself returns to its starting point, so that it appears as a fixed point of the Poincaré map.

This prescription is not directly applicable to closed orbits because they do not return to their starting point in phase space. Therefore, a trajectory starting on the surface of section will not in general intersect the surface again. To arrive at a meaningful definition of a Poincaré map, one must use two surfaces of section: the first transverse to the initial direction of the orbit, the second transverse to its final direction. A trajectory starting in the neighborhood of the closed orbit on the initial surface of section  $\Sigma_i$  will then have an intersection with the final section  $\Sigma_f$ , so that a Poincaré map is well defined. As in the case of a periodic orbit, the Poincaré map is symplectic.

Unlike with periodic orbits, the notion of a closed orbit is not invariant under canonical transformations. The distinction between position space and momentum space must therefore be kept. Let  $(q_i, p_i)$  and  $(q_f, p_f)$  be canonical coordinates on the surfaces  $\Sigma_i$  and  $\Sigma_f$  chosen so that  $q_i$  and  $q_f$  are position space coordinates in the directions perpendicular to the initial or final directions of the orbit. The origins of the coordinate systems are fixed so that the position of the nucleus is  $q_i = 0$  or  $q_f = 0$ , respectively. Closed orbits are then characterized by  $q_i = q_f = 0$ . In crossed fields three spatial dimensions must be dealt with, so that each of  $q_i, p_i, q_f, p_f$  is a two-dimensional vector. The reader may conveniently picture  $q_i$  and  $q_f$  as Cartesian coordinates, although in this case the conjugate momenta  $p_i$  and  $p_f$  diverge as the Coulomb singularity is approached. This difficulty can be overcome by means of a Kustaanheimo-Stiefel regularization [23]. Coordinates having the properties described above can then be shown to exist, as will be discussed in detail elsewhere [24, 25].

A closed orbit can start in  $\Sigma_i$  with arbitrary initial momentum  $p_i$ , but it must start in the plane  $q_i = 0$ . The Poincaré map maps this plane into a Lagrangian manifold in  $\Sigma_f$ . Closed orbits are given by the intersections of this manifold with the plane  $q_f = 0$ . In a less geometrical way of speaking, closed orbits can be described as solutions of the equation  $q_f(p_i, q_i = 0) = 0$ . A particular solution of this equation, corresponding to the orbit the construction started with, is given by  $q_f(p_i = 0) = 0$ . If the matrix  $B = \partial q_f / \partial p_i$  is non-singular at  $p_i = 0$ , this solution is locally unique and, by the implicit function theorem, will persist upon the variation of parameters. Thus, the closed orbit cannot undergo a bifurcation unless  $M = \det B = 0$ .

type	transformation	regular matrix
$F_1(q_i, q_f)$	$p_i = +\partial F_1 / \partial q_i, p_f = -\partial F_1 / \partial q_f$	$B$
$F_2(q_i, p_f)$	$p_i = +\partial F_2 / \partial q_i, q_f = +\partial F_2 / \partial p_f$	$D$
$F_3(p_i, q_f)$	$q_i = -\partial F_3 / \partial p_i, p_f = -\partial F_3 / \partial q_f$	$A$
$F_4(p_i, p_f)$	$q_i = -\partial F_4 / \partial p_i, q_f = +\partial F_4 / \partial p_f$	$C$

TABLE II: Overview of generating functions of different types (cf. [26]).

An overview of the bifurcation scenarios to be expected when  $\det B = 0$  can be obtained from a description of the possible modes of behavior of the Poincaré map. This can most conveniently be achieved if the Poincaré map is represented by a generating function [26]. The generating function can be chosen to depend on any combination of initial and final positions and momenta, as long as they form a complete set of independent coordinates. We adopt the well-known conventions of Goldstein [26] for denoting different types of generating functions, which are summarized in table II.

For a generic symplectic map, all possible sets of coordinates and momenta are independent, so that generating functions of any type exist. At a closed-orbit bifurcation, however, a degeneracy indicated by the condition that  $B = \partial q_f / \partial p_i$  be singular arises, so that care must be taken in choosing a generating function. Loosely speaking, if  $B$  is singular,  $p_i$  cannot be determined from  $q_i$  and  $q_f$ , so that it may be conjectured that no generating function of type  $F_1$  exists. To confirm this conjecture, we study a linear symplectic map

$$q_f = Aq_i + Bp_i, \quad p_f = Cq_i + Dp_i \quad (2)$$

with four matrices  $A, B, C, D$  satisfying the symplecticity conditions [27]

$$\begin{aligned} A^\top C &= C^\top A, & B^\top D &= D^\top B, & A^\top D - C^\top B &= 1, \\ AB^\top &= BA^\top, & CD^\top &= DC^\top, & AD^\top - BC^\top &= 1, \end{aligned} \quad (3)$$

where  $\top$  denotes the transpose. A generating function for the linear map (2) must be quadratic in its variables. From the ansatz

$$F_1(q_i, q_f) = \frac{1}{2} q_f^\top R q_f + q_f^\top S q_i + \frac{1}{2} q_i^\top T q_i \quad (4)$$

with matrices  $R, S, T$ , the map (2) is obtained if

$$\begin{aligned} R &= -DB^{-1}, & T &= -B^{-1\top}A, \\ S &= B^{-1\top} = DB^{-1}A - C. \end{aligned} \quad (5)$$

The two expressions given for  $S$  are equal by virtue of (3). As expected, a generating function of type  $F_1$  does not exist if  $B$  is singular. A similar calculation can be carried out for the other types of generating functions. For each type, one of the matrices  $A, B, C, D$  must be non-singular. These results are given in table II. Locally, they can be extended to non-linear maps by means of the implicit function theorem.

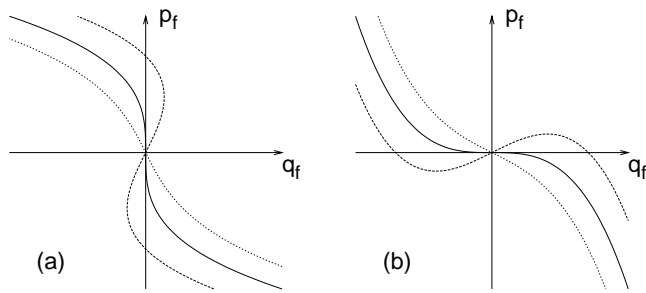


FIG. 1: Schematic plot of the Lagrangian manifold  $q_i = 0$  in  $\Sigma_f$  for the case (a)  $B = \partial q_f / \partial p_i = 0$  and (b)  $D = \partial p_f / \partial p_i = 0$ . The dashed lines indicate the position of the manifold at slightly varied parameter values. Only in case (a) additional intersections with the plane  $q_f = 0$  can arise.

Thus, at a bifurcation of closed orbits the Poincaré map generically possesses generating functions of all types except  $F_1$ . The most convenient choice is a function of type  $F_4(p_i, p_f)$ . The transformation equations associated with this type of generating function read

$$q_i = -\frac{\partial F_4}{\partial p_i}, \quad q_f = +\frac{\partial F_4}{\partial p_f}. \quad (6)$$

Closed orbits are characterized by  $q_i = q_f = 0$ . They therefore agree with the stationary points of the  $F_4$  function. The classification problem of closed-orbit bifurcation theory can thus be rephrased as the problem to determine how stationary points of a real function change upon the variation of parameters. This question is the subject of catastrophe theory [28, 29, 30].

Catastrophe theory studies smooth real-valued functions  $f(\mathbf{x})$  and  $\tilde{f}(\mathbf{x})$  defined in a neighborhood of the origin in an  $n$ -dimensional configuration space. They are said to be equivalent if there is a diffeomorphism  $\psi(\mathbf{x})$  of the configuration space so that

$$\tilde{f}(\mathbf{x}) = f(\psi(\mathbf{x})). \quad (7)$$

The coordinate transformation  $\psi$  maps the stationary points of  $\tilde{f}$  to those of  $f$ . In this sense, the distributions of stationary points of  $f$  and  $\tilde{f}$  agree qualitatively. Without loss of generality it can be assumed that  $f$  and  $\tilde{f}$  have stationary points at the origin, because any stationary point can be moved there by a coordinate transformation. After adding a constant, one has  $f(0) = 0$ .

$f$  is said to be structurally stable if any small perturbation  $\tilde{f}$  of  $f$  (i.e.  $\tilde{f}(\mathbf{x}) = f(\mathbf{x}) + \epsilon g(\mathbf{x})$  with a smooth function  $g(\mathbf{x})$  and sufficiently small  $\epsilon$ ) is equivalent to  $f$ . Notice that catastrophe theory is a purely local theory. It is concerned with the structural stability or instability of a single stationary point and the pattern of stationary points that can be generated from a structurally unstable stationary point by a small perturbation.

In the present context, non-bifurcating closed orbits correspond to structurally stable stationary points of  $F_4$ ,

because a small variation of parameters will bring about a variation of  $F_4$  which is small in the above sense and preserves the stationary point. The most elementary result of catastrophe theory states that a stationary point of a function  $f$  is structurally stable if its Hessian matrix, i.e. the matrix of second derivatives of  $f$ , is non-singular. For the linear symplectic transformation (2), the  $F_4$  generating function is

$$F_4 = \frac{1}{2} p_f^\top A C^{-1} p_f - p_f^\top C^{-1 \top} p_i + \frac{1}{2} p_i^\top C^{-1} D p_i, \quad (8)$$

so that its Hessian determinant at  $p_i = p_f = 0$  can be found to be

$$\det \text{Hess } F_4 = \frac{\det B \det D}{\det C}. \quad (9)$$

The Hessian matrix of  $F_4$  is thus singular if either  $B = \partial q_f / \partial p_i$  or  $D = \partial p_f / \partial p_i$  is. It has been shown above that bifurcations of closed orbits can only occur if  $\det B = 0$ , i.e. a bifurcating orbit corresponds to a degenerate stationary point of  $F_4$ . The case  $\det D = 0$  also leads to a degeneracy of  $F_4$ , but it cannot be associated with a closed-orbit bifurcation. This can also be understood geometrically: As illustrated in figure 1, if  $\det B = 0$ , the Lagrangian manifold given by  $q_i = 0$  is tangent to the plane  $q_f = 0$ , so that it can develop further intersections with that plane upon a small variation of parameters. If  $\det D = 0$ , the manifold is tangent to the plane  $p_f = 0$ , whence, upon a variation of parameters, it can acquire additional intersections with that plane, but not with the plane  $q_f = 0$ , so that no bifurcation of closed orbits can arise.

The discussion of stationary points with degenerate Hessian matrices, also called ‘‘catastrophes’’, is simplified considerably by the splitting lemma of catastrophe theory [30]. It states that if the dimension of the configuration space is  $n$  and a function  $f$  on the configuration space has a stationary point at the origin whose Hessian matrix has rank  $n - m$ , a coordinate system  $x_1, \dots, x_n$  can be introduced in a neighborhood of the stationary point so that

$$f(x_1, \dots, x_n) = g(x_1, \dots, x_m) + q(x_{m+1}, \dots, x_n), \quad (10)$$

where  $q$  is a non-degenerate quadratic form of  $n - m$  variables and the function  $g$  has a stationary point with zero Hessian matrix at the origin. As the non-degenerate stationary point of  $q$  is structurally stable, the behavior of the stationary points of  $f$  under a small perturbation is determined by  $g$  only. The number of relevant variables is thus only  $m$ , which is called the corank of the catastrophe. It will be assumed henceforth that a splitting according to (10) has been carried out and the non-degenerate part  $q$  is ignored, so that the Hessian matrix of  $f$  vanishes at the origin.

Under a small perturbation of the function  $f$ , a degenerate stationary point will in general split into several distinct stationary points. This process will be used to

model bifurcations of closed orbits. The degenerate stationary points relevant to bifurcation theory are those of finite codimension, i.e. those for which there are smooth functions  $g_1(\mathbf{x}), \dots, g_k(\mathbf{x})$  so that any small perturbation of  $f$  is equivalent to

$$F(\mathbf{x}) = f(\mathbf{x}) + \alpha_1 g_1(\mathbf{x}) + \dots + \alpha_k g_k(\mathbf{x}) \quad (11)$$

with suitably chosen constants  $\alpha_i$ . The function  $F(\mathbf{x})$  is called an unfolding of  $f(\mathbf{x})$ , because the degenerate stationary point of  $f$  can be regarded as a set of several stationary points that accidentally coincide and are “unfolded” by the parameters  $\alpha_i$ . The smallest value of  $k$  that can be chosen in (11) is called the codimension of  $f$ . An unfolding of  $f$  with  $k$  equal to the codimension of  $f$  is referred to as universal.

In the bifurcation problem, the generating function  $F_4$  depends on external control parameters  $\rho_1, \dots, \rho_l$  such as, e.g., the energy  $E$  or the external field strengths. If, for a critical value of the parameters,  $F_4$  has a degenerate stationary point equivalent to that of  $f$ , in a neighborhood of the critical value  $F_4$  is equivalent to the unfolding (11), where the unfolding parameters  $\alpha_i$  are smooth functions of the control parameters  $\rho_j$ . The critical parameter values themselves are characterized by the condition that all unfolding parameters vanish, i.e. by the set of equations

$$\begin{aligned} \alpha_1(\rho_1, \dots, \rho_l) &= 0, \\ &\dots \\ \alpha_k(\rho_1, \dots, \rho_l) &= 0. \end{aligned} \quad (12)$$

These are  $k$  equations in  $l$  unknowns. They can “generically” only be expected to possess a solution if  $k \leq l$ , that is, the codimension of the degenerate stationary point must not be larger than the number of external parameters. This construction introduces a notion of codimension for bifurcations of closed orbits which is entirely analogous to the codimension of bifurcations of periodic orbits: Bifurcations of a codimension higher than the number of external parameters cannot be expected to occur because they are structurally unstable. Under a small perturbation of the system they would split into a sequence of “generic” bifurcations of lower codimensions.

## B. Codimension-one generic bifurcations

The considerations of the preceding section reduce the bifurcation theory for closed orbits to the problem of determining all catastrophes having a codimension smaller than the number of external parameters. In particular, it explains why only catastrophes of finite codimension are relevant. In the crossed-fields system, the number of parameters is two, if the scaling properties are taken into account. However, we will only describe bifurcations of codimension one in the following. They suffice to describe the bifurcations encountered if a single parameter is varied while the second is kept fixed. They also give

a good impression of the codimension-two scenarios because a bifurcation of codimension two must split into a sequence of codimension-one bifurcations as soon as any of the parameters is changed.

For generic functions without special symmetries, a list of catastrophes of codimensions up to six with their universal unfoldings is readily available in the literature [28, 29, 30]. The classification of closed-orbit bifurcations presented here relies on these results.

### 1. The tangent bifurcation

There is a single catastrophe of codimension one, which has corank one and is known as the fold catastrophe. Its universal unfolding is given by

$$\Phi_a(t) = \frac{1}{3}t^3 - at, \quad (13)$$

with  $a$  denoting the unfolding parameter. The fold has two stationary points at

$$t = \pm\sqrt{a}, \quad (14)$$

where it assumes the stationary values

$$\Phi_a(\pm\sqrt{a}) = \mp\frac{2}{3}a^{3/2}. \quad (15)$$

The second derivative in the stationary points is

$$\Phi_a''(\pm\sqrt{a}) = \pm 2\sqrt{a}. \quad (16)$$

The stationary points are real if  $a > 0$ . If  $a < 0$ , there are no stationary points on the real axis, because the solutions (14) are imaginary. These complex stationary points correspond to closed ghost orbits in the complexified phase space. As  $a$  is varied, a tangent bifurcation occurs at  $a = 0$ , where two complex conjugate ghost orbits turn into two real orbits or vice versa.

All qualitative features of the bifurcation are described by the normal form (13). The stationary points, i.e. the closed orbits, initially move apart as  $\sqrt{a}$ . A more detailed connection between the properties of the normal form and the closed orbits can be made in the context of uniform semiclassical approximations. The difference between the stationary values gives the action difference between the closed orbits, whereas the second derivatives – or, if the normal form has corank greater than one, the Hessian determinants – at the stationary points are proportional to a parameter  $M$  describing the stability of the closed orbit (see [21, 24] for details). All these quantities are shown in figure 2. When they are compared to the corresponding quantities calculated for an actual bifurcation in section V, the qualitative agreement will become clear.

The fold catastrophe (13) describes the generation of two closed orbits in a tangent bifurcation. As this is the only generic catastrophe of codimension one, it follows

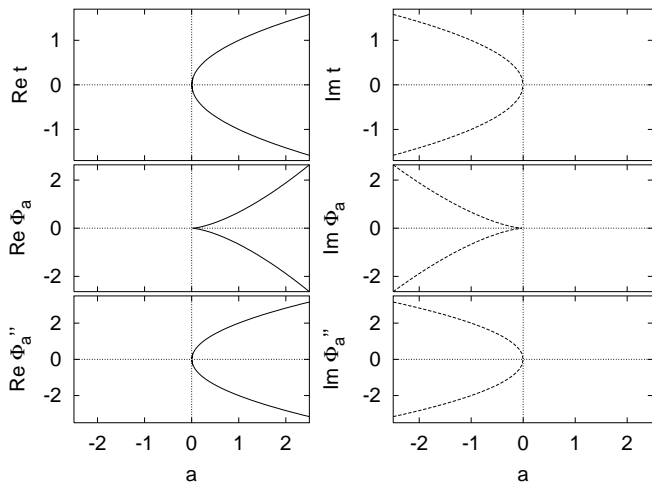


FIG. 2: The positions of stationary points, stationary values and second derivatives in the fold catastrophe. Solid lines indicate real stationary points, dashed lines complex stationary points. Dotted lines are coordinate axes.

that the tangent bifurcation is the only possible type of closed-orbit bifurcations. In particular, once it has been generated a closed orbit cannot split into several orbits, as periodic orbits typically do. However, this statement needs some modification due to the presence of reflection symmetries in the crossed-fields system.

## 2. The pitchfork bifurcation

If the orbit under study is symmetric under one of the reflections, i.e. it is a singlet or a doublet orbit, the generating function  $F_4$  in the neighborhood of this orbit must also possess this reflection symmetry. By this constraint, several of the elementary catastrophes are excluded altogether. For others, the codimension is reduced because the unfolding can only contain symmetric terms.

One additional catastrophe of codimension one arises, viz. the symmetrized version of the cusp catastrophe

$$\Phi_a(t) = \frac{1}{4}t^4 - \frac{1}{2}at^2. \quad (17)$$

This normal form possesses the reflection symmetry  $t \mapsto -t$ , so that the origin is mapped onto itself under the symmetry transformation. There is a stationary point at the origin for all values of the parameter  $a$ , corresponding to a closed orbit which is invariant under the reflection. Additional stationary points are located at

$$t = \pm\sqrt{a}. \quad (18)$$

They are real if  $a > 0$  and are mapped onto each other under a reflection. Thus, the symmetric cusp (17) describes a pitchfork bifurcation at  $a = 0$ , where two asymmetric orbits bifurcate off a symmetric orbit, generating a quartet from a doublet or a doublet from a singlet.

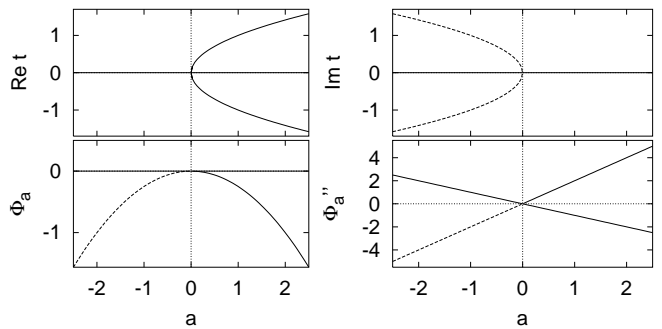


FIG. 3: The positions of stationary points, stationary values and second derivatives in the cusp catastrophe. Solid lines indicate real stationary points, dashed lines complex stationary points. Dotted lines are coordinate axes. Note that stationary values and second derivatives are real even for complex stationary points.

The stationary values at the asymmetric stationary points are given by

$$\Phi_a(\pm\sqrt{a}) = -\frac{1}{4}a^2, \quad (19)$$

the second derivative is

$$\Phi_a''(\pm\sqrt{a}) = 2a. \quad (20)$$

Both the stationary values and the values of the second derivative are real even for  $a < 0$ , when the stationary points themselves are complex. Therefore, these stationary points correspond to ghost orbits having real actions and stability determinants. The existence of this remarkable type of ghost orbits is again a consequence of the reflection symmetry: As the stationary points (18) are imaginary, the reflection  $t \mapsto -t$  changes a stationary point and its stationary value into their complex conjugates. On the other hand, the stationary values are invariant under the reflection, so they must be real. A ghost orbit having this symmetry property will be referred to as a symmetric ghost orbit.

The characteristic quantities of the symmetric cusp catastrophe are shown in figure 3 as a function of  $a$ . Again, they describe the qualitative behavior of the bifurcating orbits close to the bifurcation. It should be noted that the stationary values (19) are negative for all values of  $a$ , so that for a bifurcation described by (17), the actions of the asymmetric orbits must be smaller than those of the symmetric orbit. An alternative bifurcation scenario is described by the dual cusp, viz. the negative of (17). The dual cusp is inequivalent to the regular cusp, but the scenario it describes agrees with the above except that the stationary values and the second derivatives change their signs, so that the actions of the asymmetric orbits are now larger than that of the symmetric orbit.

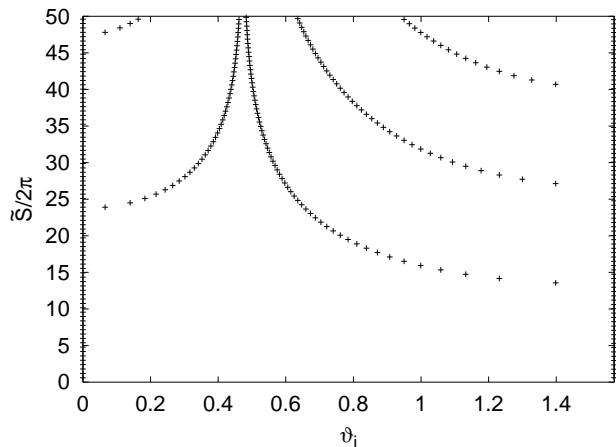


FIG. 4: Scaled actions  $\tilde{S}$  as functions of the starting angles  $\vartheta_i$  of closed orbits in the DKP for  $\tilde{E} = -1.4$ .

#### IV. CLOSED ORBITS IN THE DIAMAGNETIC KEPLER PROBLEM

As a basis for the description of closed orbits in the crossed-fields hydrogen atom, we will choose the closed orbits in the diamagnetic Kepler problem (DKP), i.e. in the hydrogen atom in a pure magnetic field. For these orbits a complete classification is available [3, 4, 5, 6, 7, 8]. It will now be recapitulated briefly.

For low scaled energies  $\tilde{E} \rightarrow -\infty$ , there are two fundamental closed orbits: In one case, the electron leaves the nucleus parallel to the magnetic field until the Coulomb attraction forces it back. This orbit is purely Coulombic because the electron does not feel a Lorentz force when moving parallel to the magnetic field. The second closed orbit lies in the plane perpendicular to the magnetic field. Its shape is determined by the combined influences of the Coulomb and magnetic fields.

Due to time-reversal invariance, both elementary orbits possess arbitrary repetitions. As the scaled energy increases, each repetition of an elementary orbit undergoes a sequence of bifurcations labelled by an integer  $\nu = 1, 2, 3, \dots$  in order of increasing bifurcation energy. The orbits born in these bifurcations can be characterized by the repetition number  $\mu$  of the bifurcating orbit and the bifurcation number  $\nu$ . They are referred to [3] as vibrators  $V_\mu^\nu$  if they bifurcate out of the orbit parallel to the magnetic field and as rotators  $R_\mu^\nu$  if they bifurcate out of the orbit perpendicular to  $\mathbf{B}$ .

Further bifurcations create additional orbits from the  $V_\mu^\nu$  and  $R_\mu^\nu$  or “exotic” orbits not related to one of the two fundamental orbits. These orbits are of importance at scaled energies higher than those considered in this work, so that they will not be discussed further. For the scaled energy  $\tilde{E} = -1.4$ , the scaled actions and starting angles of the closed orbits are presented in figure 4. It can be seen that only orbits fitting into the classification scheme described above are present. Furthermore, orbits

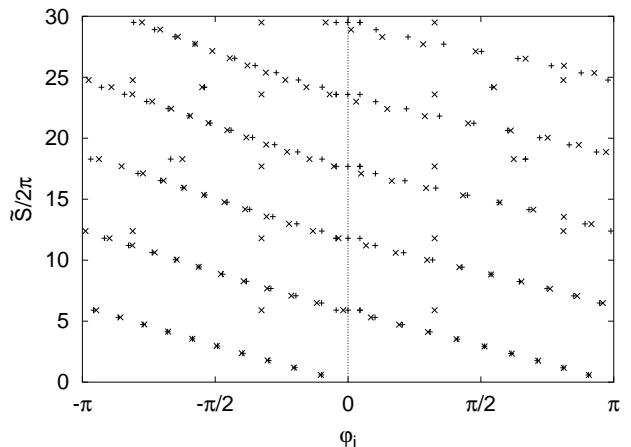


FIG. 5: Scaled actions  $\tilde{S}$  and azimuthal starting angles  $\varphi_i$  for planar orbits at  $\tilde{E} = -1.4$  and  $\tilde{F} = 0.03$  (+ symbols) and  $\tilde{F} = 0.05$  ( $\times$  symbols).

having a common bifurcation number  $\nu$  lie on a smooth curve in the plot. For this reason, we will refer to orbits characterized by a fixed  $\nu$  as a series of rotators or vibrators, respectively, and call  $\nu$  the series number.

#### V. CLOSED ORBIT BIFURCATION SCENARIOS

In the presence of a pure magnetic field, the atomic system possesses a rotational symmetry around the field axis. As a consequence, all closed orbits except for the orbit parallel to the magnetic field occur in continuous one-parameter families obtained by rotating a single orbit around the symmetry axis. When a perpendicular electric field is added, the rotational symmetry is broken. Out of each family, only two orbits survive [31], or, in other words, each family of orbits splits into two independent orbits.

##### A. Planar orbits

The splitting of a family of orbits upon the introduction of an electric field can most clearly be seen for planar orbits, i.e. for orbits lying in the plane perpendicular to the magnetic field. Due to the Z-symmetry, this plane is invariant under the dynamics. Thus, the initial direction of an orbit can be specified by means of the azimuthal angle  $\varphi_i$  only.

Figure 5 shows the actions and initial directions of the planar orbits for a scaled energy of  $\tilde{E} = -1.4$  and scaled electric field strengths  $\tilde{F} = 0.03$  and  $\tilde{F} = 0.05$ . At  $\tilde{F} = 0$ , the orbits bifurcate off a certain repetition of the planar closed orbit of the diamagnetic Kepler problem. For low  $\tilde{F}$  they can therefore be assigned a repetition number. It can clearly be discerned in figure 5 from the actions of

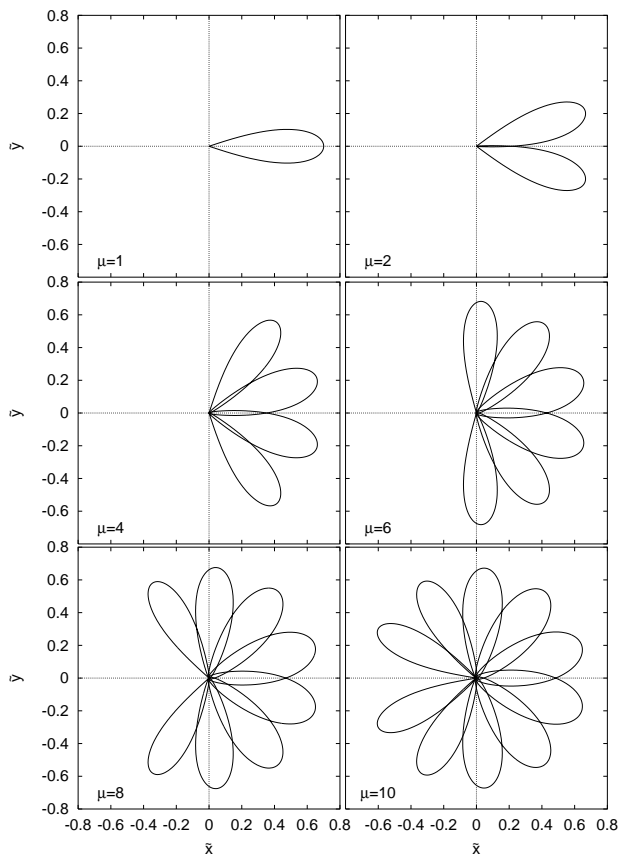


FIG. 6: Elementary planar closed orbits at  $\tilde{E} = -1.4$  and  $\tilde{F} = 0.05$ .  $\mu$  is the repetition number. The orbits are symmetric with respect to the  $x$ -axis, in particular,  $\varphi_i = -\varphi_f$ .

the orbits.

As expected from the theory of the rotational symmetry breaking [31], there are two orbits for each repetition number, and they start in opposite directions from the nucleus. Moreover, the starting angle varies linearly with the repetition number. These findings are illustrated in figure 6, where for a few low repetition numbers one of the two orbits is shown. It can be seen that the orbits consist of more and more “loops” and that the starting angle increases regularly. The shapes are symmetric with respect to the  $x$ -axis because the orbits are invariant under the  $T$ -transformation, i.e. these orbits are singlets.

A few orbits in figure 5 do not fit into this simple scheme. A closer inspection reveals that these orbits are not singlets, but  $Z$ -doublets, and indeed they obviously occur in pairs. They are generated by symmetry-breaking pitchfork bifurcations from singlet orbits. Figure 7 presents the orbital parameters for closed orbits involved in a bifurcation of this kind. The panels show the real and imaginary parts of the starting angles  $\varphi_i$  of the orbits, the scaled actions  $\tilde{S}$  and the stability determinant  $M = \det(\partial q_f / \partial p_i)$  (see section III A), whose zeros indicate the occurrence of a bifurcation and that also plays an important role in closed-orbit theory [21]. These plots should be compared to figure 3, which displays the

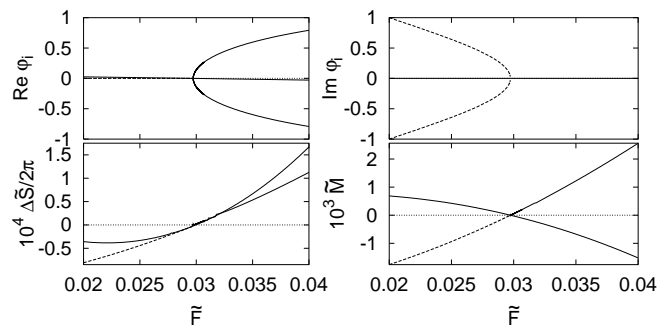


FIG. 7: Orbital parameters close to a pitchfork bifurcation creating a  $Z$ -doublet of closed orbits from a singlet at  $\tilde{E} = -1.4$ , repetition number  $\mu = 10$ .  $\varphi_i$  is the azimuthal starting angle,  $\tilde{S}$  the scaled action and  $M$  the scaled stability determinant,  $\Delta\tilde{S} = \tilde{S} - 2\pi \times 5.898159$  was introduced for graphical purposes. Thick solid lines: singlet orbit, thin solid lines: doublet orbits, dashed line: ghost orbits symmetric with respect to complex conjugation. Dotted lines indicate coordinate axes.

scenario described by the symmetric cusp catastrophe. The qualitative agreement between the catastrophe theory predictions and the numerical findings is evident.

A closer look at the asymmetric orbits reveals that they have equal initial and final azimuthal angles  $\varphi_i = \varphi_f$ , i.e. they are not only closed, but also periodic orbits. The initial and final angles of these orbits satisfy  $\varphi_i^{(1)} = -\varphi_f^{(2)}$  because they are symmetry partners and  $\varphi_i^{(2)} = \varphi_f^{(2)}$  because they are periodic. Thus, they must fulfil  $\varphi_i^{(1)} = -\varphi_i^{(2)}$ . At the bifurcation, the initial angles of the two orbits must coincide, so that a bifurcation can only take place when  $\varphi_i = 0$  or  $\varphi_i = \pi$ , and it actually does take place every time one of these conditions is fulfilled. This process can be seen in figure 5, e.g., at  $S/2\pi \approx 25$ : At  $\tilde{F} = 0.03$ , the symmetric orbit has not yet crossed the line  $\varphi_i = \pi$ , so that no bifurcation has occurred. At  $\tilde{F} = 0.05$ , this line has been crossed and two asymmetric orbits have been created.

As the electric field strength is increased, the dependence of the starting angle on the repetition number ceases to be linear. Instead, the curves interpolating the functions  $\tilde{S}(\varphi_i)$  start to develop humps, so that at certain values of  $\tilde{S}$ , i.e. at certain repetition numbers, more than two possible values of  $\varphi_i$  exist. This development is illustrated in figure 8. The humps indicate the occurrence of tangent bifurcations generating additional pairs of singlet orbits. This is the type of bifurcation described by the fold catastrophe (13). Orbital parameters for orbits involved in a bifurcation of this kind are shown in figure 9. As for the pitchfork bifurcation, a comparison of that figure to the catastrophe theory predictions in figure 2 reveals that the bifurcation is well described qualitatively by the fold catastrophe.

Once additional singlet orbits have been generated in a tangent bifurcation, doublet orbits can be generated by

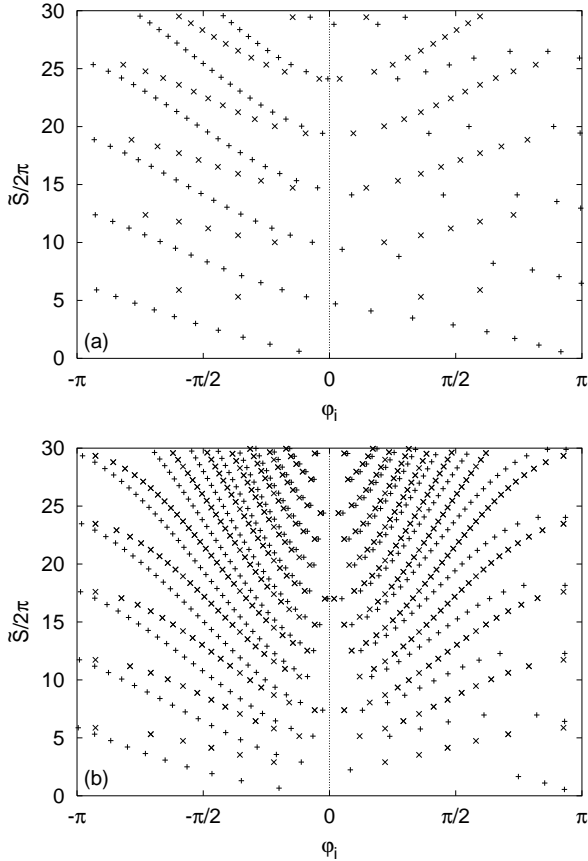


FIG. 8: Scaled actions and azimuthal starting angles for planar orbits at  $\tilde{E} = -1.4$  and (a)  $\tilde{F} = 0.2$ , (b)  $\tilde{F} = 0.5$ . Singlets are indicated by + symbols, Z-doublets by  $\times$  symbols.

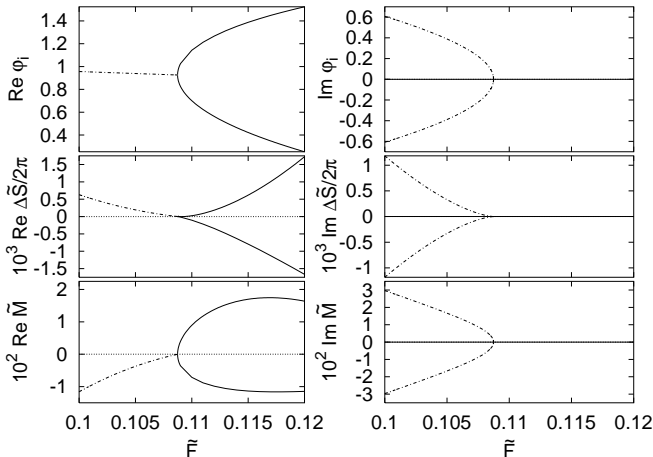


FIG. 9: Orbital parameters close to a tangent bifurcation of planar orbits at a  $\tilde{E} = -1.4$  and a winding number of  $\mu = 45$ . ( $\Delta\tilde{S} = \tilde{S} - 2\pi \times 26.512735$ .) Solid lines: real orbits, dashed-dotted lines: ghost orbits.

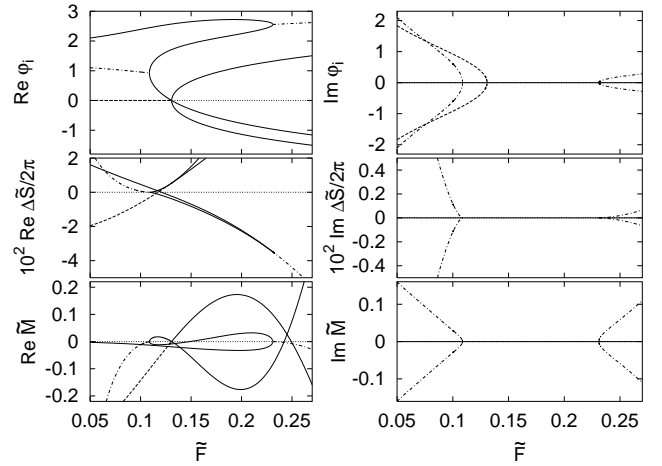


FIG. 10: The bifurcation scenario taking place in the neighborhood of the tangent bifurcation shown in figure 9. ( $\Delta\tilde{S} = \tilde{S} - 2\pi \times 26.2735$ ). Thick solid lines: real singlet orbits, thin solid lines: real Z-doublet orbits, dashed lines: symmetric ghost orbits, dashed-dotted lines: asymmetric ghost orbits. Dotted lines are coordinate axes.

pitchfork bifurcations in the same way as from the original singlet orbits, i.e. a bifurcation will occur whenever a singlet orbit crosses one of the lines  $\varphi_i = 0$  or  $\varphi_i = \pi$ . This is illustrated in figure 10, which presents the tangent bifurcation already shown in figure 9 at  $\tilde{F} \approx 0.11$ . At  $\tilde{F} = 0.135$ , one of the orbits thus generated crosses the line  $\varphi_i = 0$ , and two doublet orbits are created from it. Together, the two bifurcations form what Wang and Delos [18] call the “normal sequence” of bifurcations, whereas a pitchfork bifurcation of a singlet orbit generated at  $\tilde{F} = 0$ , which is not preceded by a tangent bifurcation, is called a “truncated series”. These authors introduce an integrable model Hamiltonian to explain why this kind of sequences can often be observed for planar orbits. The bifurcation theory of sections III A and III B sheds new light on this question, suggesting that normal sequences can actually be expected to occur even more generally than surmised by Wang and Delos. In particular, although the crossed-fields system is close to integrable at the field strengths considered here, integrability is not needed to make pitchfork bifurcations a generic phenomenon. Instead, the presence of a reflection symmetry suffices to reduce its codimension from two to one. The sequence of a tangent and a pitchfork bifurcation, represented as a sequence of a fold and a symmetric cusp catastrophe, can be regarded as an unfolding of the symmetrized version of the butterfly catastrophe [20, 29]

$$\Phi_{a,b}(t) = \frac{1}{6}t^6 - \frac{1}{4}at^4 - \frac{1}{2}bt^2, \quad (21)$$

which is of codimension two, so that its unfolding can be expected to occur frequently in codimension one.

A third bifurcation can be discerned in figure 10: At  $\tilde{F} \approx 0.225$ , a singlet orbit generated at  $\tilde{F} = 0$  and a sin-

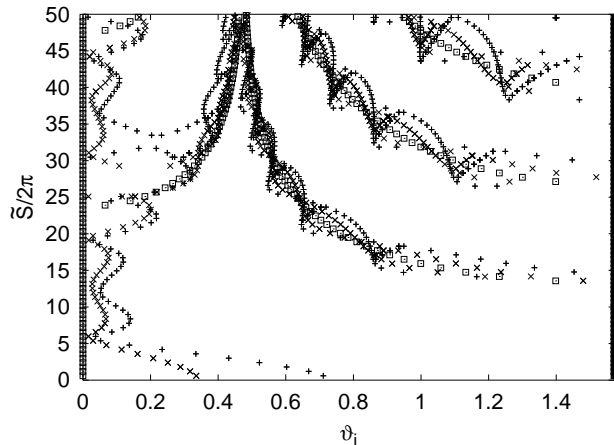


FIG. 11: Scaled actions and polar starting angles of closed orbits at  $\tilde{E} = -1.4$  and  $\tilde{F} = 0$  (pure magnetic field, + symbols),  $\tilde{F} = 0.05$  (× symbols) and  $\tilde{F} = 0.1$  (□ symbols). Due to the Z-symmetry, the figure should be extended to be symmetric with respect to the line  $\vartheta_i = \pi/2$ .

glet orbit generated in the tangent bifurcation discussed above collide and are destroyed. This is an instant of an inverse tangent bifurcation, which can be described by the fold catastrophe in the same way as the “regular” tangent bifurcation. It forms the third building block for the bifurcation scenario changing the pattern of planar orbits as the electric field strength is increased.

Besides the three bifurcations described above, in figure 10 three further zeros of the stability determinant  $M$  occur for certain real orbits, indicating the presence of even more bifurcations. These bifurcations involve non-planar orbits, i.e. they are pitchfork bifurcations breaking the Z-symmetry all planar orbits possess. They will be discussed further in subsequent sections. At the moment it suffices to note that in this scenario six individual bifurcations take place in a comparatively small interval of the electric field strength. This is the first example of a phenomenon to be encountered repeatedly: In the crossed-fields hydrogen atom bifurcations of closed orbits abound, exacerbating both the classical and the semiclassical treatment of the dynamics.

## B. Non-planar orbits

The transition from the rotationally-symmetric case of a pure magnetic field to crossed fields occurs for non-planar orbits in much the same way as for planar orbits. As soon as a small perpendicular electric field is present, a one-parameter family of DKP orbits is destroyed and splits into two isolated closed orbits. These orbits start in opposite directions with respect to the electric field, so that their azimuthal starting angles  $\varphi_i$  differ by  $\pi$ , in complete analogy with what was shown in figure 5. An additional complication arises because the polar starting

angle  $\vartheta_i$  is no longer bound to the fixed value  $\pi/2$ , so that the two orbits will in general have different  $\vartheta_i$ . Figure 11 presents the polar starting angles and the scaled actions of the closed orbits for the scaled energy  $\tilde{E} = -1.4$  in a pure magnetic field and for two different perpendicular electric field strengths. Only angles  $\vartheta_i \leq \pi/2$  need to be shown because orbits with  $\vartheta_i > \pi/2$  can be obtained by a Z-reflection. It is obvious from the figure how a family of orbits splits in two isolated orbits and the two orbits move apart as the electric field strength is increased. This process takes place in the same way for both rotator and vibrator orbits.

An exceptional role is played by the DKP orbit parallel to the magnetic field. This orbit is isolated even in a pure magnetic field. In the presence of a perpendicular electric field it is distorted and torn away from the magnetic field axis, but it remains isolated rather than splitting into two orbits. This process is also apparent from figure 11. Notice again that closed orbits in crossed fields do not possess repetitions. Any repetition of the parallel DKP orbit gives rise to a closed orbit in crossed fields (for sufficiently small  $\tilde{F}$ ), but these orbits are not repetitions of each other. They have, in particular, different starting angles.

The symmetries of the closed orbits are worth noting. All non-planar orbits described so far are doublets. More precisely, the vibrator orbits are T-doublets, i.e. they are invariant under the T operation. Their initial and final polar angles are small, as the orbits are mainly directed along the magnetic field axis.

For the rotator orbits the situation is more complex. Their main component is the motion in the plane perpendicular to the magnetic field, whereas the  $z$ -component is comparatively small. They have, therefore, initial and final polar angles close to  $\pi/2$ , so that it is conceivable that they can start at an angle  $\vartheta_i < \pi/2$  “above” the  $x$ - $y$ -plane and return at  $\vartheta_f > \pi/2$  “below” that plane. This is in fact the case for the rotators of the first series. They turn out to be C-doublets.

The second series of rotators contains orbits which, in the case of a pure magnetic field, are composed of a first-series orbit and its Z-reflected counterpart. The orbits of the second series therefore have  $\vartheta_i = \vartheta_f$  and are T-doublets. By the same token, orbits of the third series return “below” the  $x$ - $y$ -plane again and are C-doublets, and higher series of rotators alternately contain T-doublets and C-doublets.

The distribution of symmetries is illustrated in figure 12(a). It extends the data given in figure 11 to longer orbits and classifies the orbits according to their symmetries.

So far, only orbits present at arbitrarily low electric field strengths have been described. As the electric field strength increases, further bifurcations occur. Their general pattern can be identified in figures 11 and 12(a). The most obvious consequence of the bifurcations is the appearance of quartet orbits in each series of both rotator and vibrator orbits. They are generated by pitchfork bi-

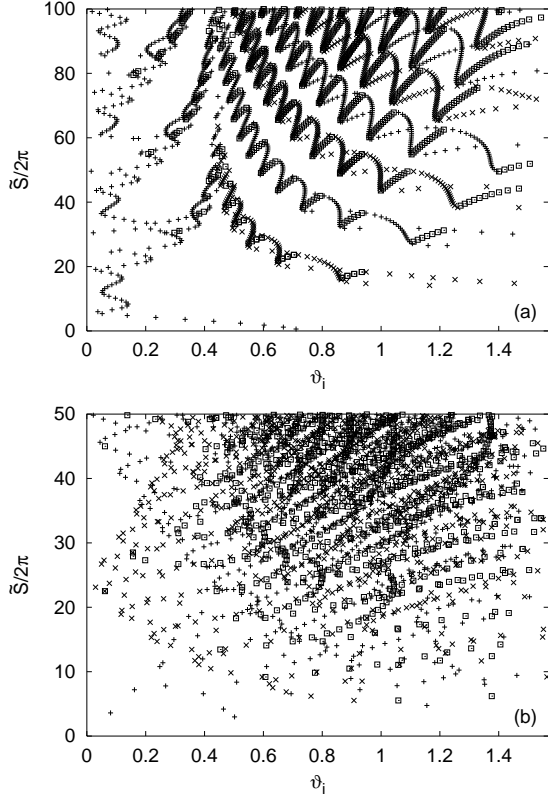


FIG. 12: Scaled actions and polar starting angles of closed orbits at  $\tilde{E} = -1.4$  and (a)  $\tilde{F} = 0.1$ , (b)  $\tilde{F} = 0.6$ . Orbits are classified according to their symmetries: T-doublets are indicated by + symbols, C-doublets by  $\times$  symbols, quartets by  $\square$  symbols. Planar orbits (Z-doublets and singlets) are omitted. Notice that the range of actions shown is smaller in (b).

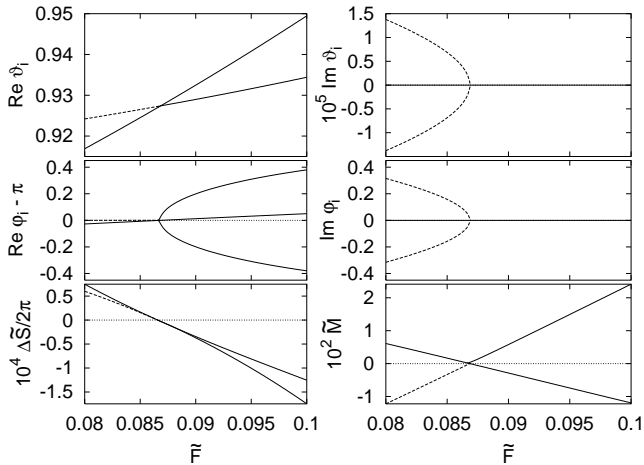


FIG. 13: Orbital parameters close to a pitchfork bifurcation of a first-series rotator and a repetition number of  $\mu = 38$ . The bifurcation creates a quartet of orbits from a C-doublet. ( $\Delta\tilde{S} = \tilde{S} - 2\pi \times 18.297822$ .)

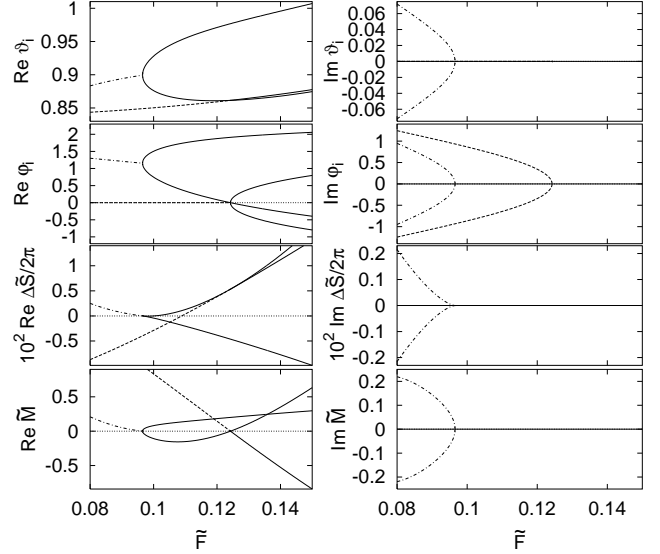


FIG. 14: “Normal sequence” of bifurcations for non-planar rotator orbits of the second series and a repetition number of  $\mu = 54$ . ( $\Delta\tilde{S} = \tilde{S} - 2\pi \times 31.84035$ .)

furcations from the adjacent doublet orbits. As figure 13 reveals if it is compared to figure 7, this bifurcation is very similar to a pitchfork bifurcation of planar orbits. A difference arises because, due to the absence of Z-symmetry, the angle  $\vartheta_i$  is not restricted to a fixed value. As the C-symmetry to be broken concerns the azimuth angles, it still is predominantly the angle  $\varphi_i$  that shows a square root behavior at the bifurcation and obtains an imaginary part when ghost orbits exist. Nevertheless the polar angle  $\vartheta_i$  also acquires a small imaginary part. The real part of  $\vartheta_i$  apparently behaves linear close to the bifurcation, although for electric field strengths above the critical value a square root behavior must be present. It is too small to be seen in the figure. Even though in quantitative terms the  $\vartheta$ -direction is only marginally involved in the bifurcation, its presence has the important consequence that the quartet orbits are no longer constrained to be periodic. As the distance from the bifurcation is increased, the periodicity condition  $\varphi_i = \varphi_f$  is increasingly, albeit slowly, violated. The same features can be found for the bifurcations introducing the quartet orbits into the vibrator series.

The second important type of bifurcations is a tangent bifurcation introducing new doublet orbits into the series. The occurrence of this phenomenon can be noticed in figure 11, if the numbers of orbits of a given repetition number are compared for different electric field strengths. An example of this bifurcation is given in figure 14. The tangent bifurcation involves both angles to roughly equal extent. The two doublet orbits thus generated are implanted into the regular pattern of their series, so that one of them subsequently undergoes a pitchfork bifurcation which creates a quartet. This phenomenon is entirely analogous to the “normal sequence” of bifurca-

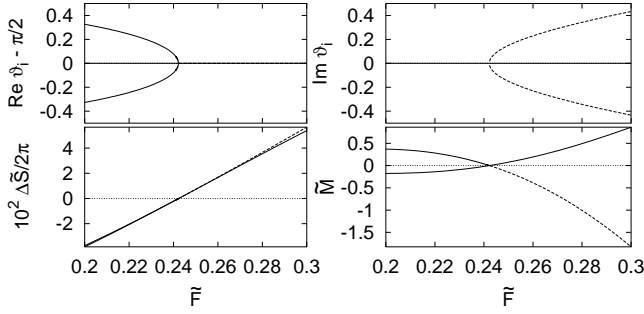


FIG. 15: Destruction of T-doublet orbits in a collision with a singlet orbit. ( $\Delta\tilde{S} = \tilde{S} - 2\pi \times 27.60324$ .)

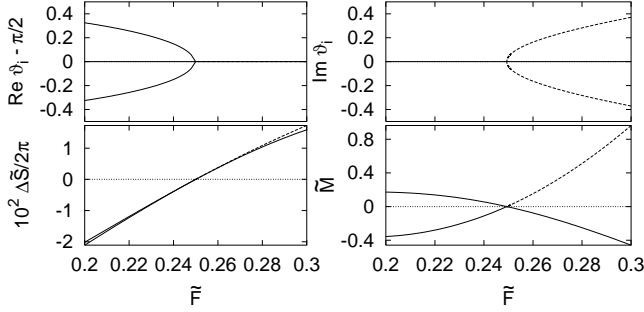


FIG. 16: Destruction of quartet orbits in a collision with Z-doublet orbits. ( $\Delta\tilde{S} = \tilde{S} - 2\pi \times 26.569655$ .)

tions that was found for planar orbits, except that the quartet orbits thus generated are not periodic.

As the electric field strength increases, the rotator orbits of a given series are torn apart and span an ever wider interval of  $\vartheta_i$ . Those orbits moving towards higher values of  $\vartheta_i$  eventually hit the plane  $\vartheta_i = \pi/2$ , where they collide with their Z-reflected partners and are destroyed. One might suspect the destruction of the two orbits to occur in a tangent bifurcation, but from the discussion of section III B it is clear that a tangent bifurcation can only create or destroy orbits having different actions, so that it can never involve two orbits related by a symmetry transformation. Thus, the bifurcation must be of pitchfork type, and it must involve a Z-symmetric planar orbit. Depending on whether the non-planar orbits colliding with the plane are doublets or quartets, the planar orbit must be a singlet or a Z-doublet, respectively. If the destruction scenario is regarded in the direction of decreasing field strengths, it appears as the creation of orbits with broken Z-symmetry from an orbit possessing this symmetry. It is therefore the Z-breaking analogue of the T- and C-symmetry breaking bifurcations described above. As this type of bifurcation involves a planar orbit, it must give rise to a zero in the stability determinant  $M$  of the planar orbit. In fact, the examples given in figures 15 and 16 for both the destruction of a doublet and a quartet are two of the three bifurcations whose presence was inferred from figure 10 the discussion of the planar orbits.

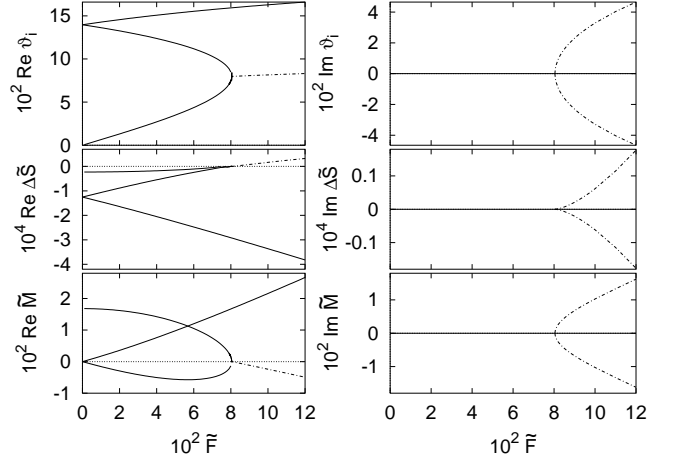


FIG. 17: Simple bifurcation scenario for vibrator orbits of repetition number  $\mu = 41$ . ( $\Delta\tilde{S} = \tilde{S} - 2\pi \times 24.50221$ .)

The scenario just described is not restricted to rotator orbits. As can be seen in figure 11, the short vibrator orbits can, even at low electric field strengths, reach rather high values of  $\vartheta_i$ . At  $\tilde{F} = 0.15550$  the first of them collides, at  $\vartheta_i = \pi/2$ , with its Z-reflected counterpart and is annihilated. This is a pitchfork bifurcation in which one of the planar orbits with repetition number  $\mu = 1$  takes part. Similarly, longer vibrators are destroyed in collisions with planar rotators of the appropriate repetition numbers. This example demonstrates that the distinction between vibrators and rotators, which was borrowed from the case of vanishing electric field, does not apply, strictly speaking, if an electric field is present. Although it is generally useful for rather high electric field strengths, it can fail in some instances. This is clearly the case when a bifurcation involves both vibrator and rotator orbits.

A collision with the plane perpendicular to the magnetic field occurs only for vibrators of low repetition numbers, and only for vibrators that descend from the orbit parallel to the magnetic field. For longer orbits, the usual scenario is different. At low electric field strength there is, for sufficiently high repetition numbers, one orbit stemming from the orbit parallel to the magnetic field and one or several pairs of orbits created from non-parallel vibrators. It can be seen in figure 11, however, that for certain repetition numbers two of these orbits can be missing. This happens when the descendant of the parallel orbit and one of the other vibrators annihilate in a tangent bifurcation. A simple example of how this can come about is provided by the orbits with the repetition number  $\mu = 41$ . Their bifurcations are illustrated in figure 17. Two of the orbits obviously bifurcate from a common family at  $\tilde{F} = 0$ , whereas the orbit proceeding from the parallel orbit is isolated there and starts at  $\vartheta_i = 0$ . It then merges with one of the other orbits in a tangent bifurcation to form a pair of ghost orbits.

This bifurcation is as simple as one could expect. For

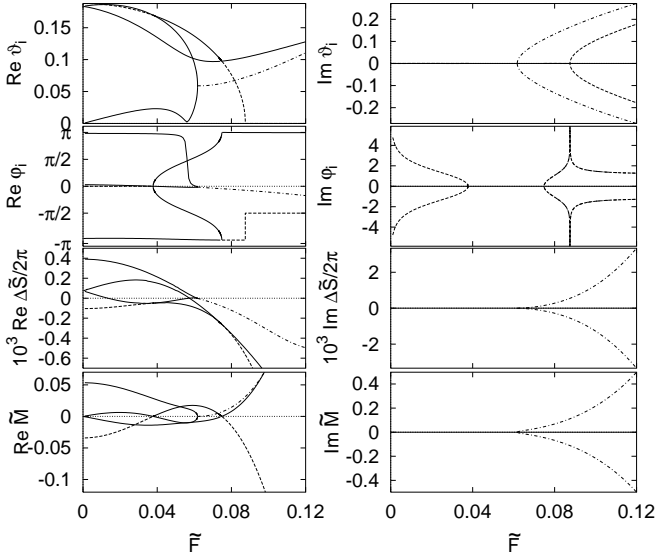


FIG. 18: Complicated bifurcation scenario for vibrator orbits of repetition number  $\mu = 42$ . ( $\Delta\tilde{S} = \tilde{S} - 2\pi \times 25.09941$ .)

the neighboring vibration number  $\mu = 42$  the scenario is more complicated. It is illustrated in figure 18. In this case, one of the orbits generated in the rotational symmetry breaking at  $\tilde{F} = 0$ , which is a T-doublet, undergoes a pitchfork bifurcation and gives birth to a quartet of orbits before it annihilates with the descendant of the parallel orbit. The quartet then collides with the third, leftover T-doublet and is destroyed in a second pitchfork bifurcation.

Corresponding to the three elementary bifurcations, there are three ghost orbits involved in the scenario. For one of them, the starting angles  $\vartheta_i$  and  $\varphi_i$  show a peculiar behavior at the electric field strength  $\tilde{F}_0 = 0.08750$ : Whereas  $\vartheta_i$  exhibits a square root behavior, changing from nearly real to nearly imaginary values, the real part of  $\varphi_i$  changes discontinuously by  $\pi/2$ , and the imaginary part of  $\varphi_i$  seems to diverge. Neither the action nor the stability determinant of the orbit, on the contrary, show any kind of special behavior. In particular,  $\tilde{M}$  is non-zero, so that there cannot be a bifurcation of the ghost orbit.

The Cartesian components of the unit vector  $\mathbf{s}$  in the starting direction are given in figure 19. For all of them either the real or the imaginary parts are small, so that their numerical calculation is hard. Nevertheless, to within the numerical accuracy all components are smooth at  $\tilde{F}_0$ , although the angles  $\vartheta_i$  and  $\varphi_i$  used to calculate them are not. Thus, the singularity must be due to the transformation from Cartesian to angular coordinates. In the real case it is obvious that the  $(\vartheta, \varphi)$  coordinate chart is singular at  $\vartheta = 0$ . To elucidate the details in the case of ghost orbits, assume a model situation where  $s_z = \cos \vartheta_i$  is exactly real and  $s_z = 1$  at  $\tilde{F} = \tilde{F}_0$ . For ghost orbits,  $s_z$  is not bound to be smaller than 1, so that generically, to first order in  $\varepsilon = \tilde{F} - \tilde{F}_0$ ,

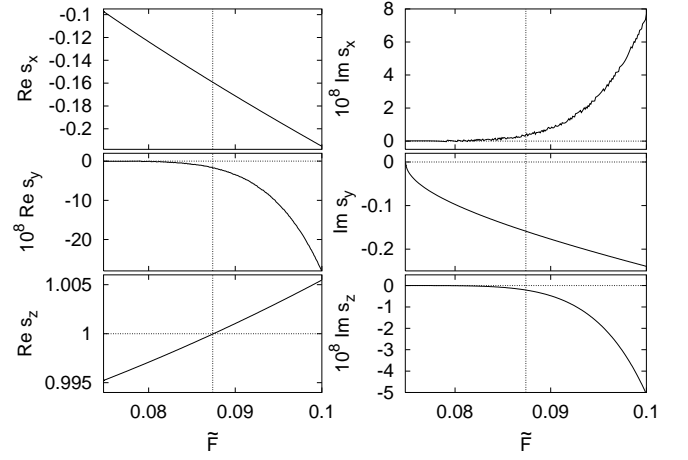


FIG. 19: Cartesian components of the unit vector  $\mathbf{s}$  specifying the starting direction of the ghost orbit ( $s_x = \sin \vartheta_i \cos \varphi_i$ ,  $s_y = \sin \vartheta_i \sin \varphi_i$ ,  $s_z = \cos \vartheta_i$ ). Vertical dotted lines mark the field strength  $\tilde{F}_0 = 0.08750$  where the singularity of  $\text{Im } \varphi_i$  is encountered.

cos  $\vartheta_i - 1 \propto \varepsilon$ . Therefore,  $\vartheta_i \propto \sqrt{\varepsilon}$  shows a square root behavior and changes from purely real to purely imaginary values. At the same time,  $\sin \vartheta_i \propto \sqrt{\varepsilon}$  has a zero, so that for  $s_x = \sin \vartheta_i \cos \varphi_i$  and  $s_y = \sin \vartheta_i \sin \varphi_i$  to assume finite values,  $\sin \varphi_i$  and  $\cos \varphi_i$  must diverge as  $\varepsilon^{-1/2}$ . This is only possible if the imaginary part of  $\varphi_i$  is large. More precisely, if  $\text{Im } \varphi_i > 0$  is assumed to be large,  $\sin \varphi_i$  and  $\cos \varphi_i$  are proportional to  $e^{-i\varphi_i}$ , whence

$$\varphi_i = \frac{1}{2i} \ln \varepsilon + \mathcal{O}(\varepsilon^0) \quad (22)$$

achieves the desired divergence of  $\sin \varphi_i$  and  $\cos \varphi_i$ . Now  $\text{Re } \ln \varepsilon = \ln |\varepsilon|$  diverges at  $\varepsilon = 0$ , whereas  $\text{Im } \ln \varepsilon$  changes discontinuously from 0 to  $\pm\pi$ , depending on what branch of the logarithm is chosen. This behavior results in the observed divergence of  $\text{Im } \varphi_i$  and a discontinuous jump in  $\text{Re } \varphi_i$  of size  $\pi/2$ .

In the actual scenario  $s_z$  will not be exactly equal to 1 at  $\tilde{F}_0$  because this is a situation of real codimension two. However, if  $\text{Im } s_z$  is small, the singular behavior described above will be closely approximated. Indeed, a closer look at  $\vartheta_i$  (see figure 20) reveals that it is actually smooth, but close to  $\tilde{F} = \tilde{F}_0$  it changes extremely rapidly from almost real to predominantly imaginary values. Similarly, the real part of  $\varphi_i$  is smooth, although it changes over an even smaller range of  $\tilde{F}$ . From the numerical data it cannot be determined if  $\text{Im } \varphi_i$  is also smooth or actually diverges. From the above discussion it is clear that it must be smooth, because the coordinate singularity at  $\vartheta_i = 0$  is not actually encountered.

It should be noted that the singularity described here can occur for ghost orbits only. In the real case, as the pole  $\vartheta_i = 0$  on the real unit sphere (which still has codimension two) is approached, both  $s_x$  and  $s_y$  must vanish instead of assuming finite values, so that no divergences

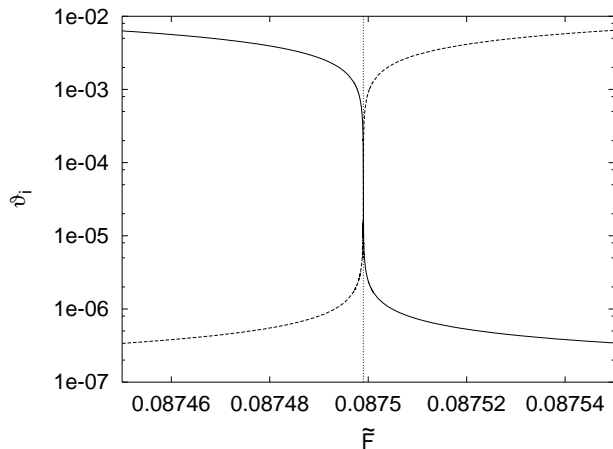


FIG. 20: The starting angle  $\vartheta_i$  of the ghost orbit close to the coordinate singularity. Solid line: real part, dashed line: imaginary part. Note the logarithmic scale.

of any kind are required.

## VI. THE CLASSIFICATION OF CLOSED ORBITS

The fundamental classification scheme used in the above description of closed orbit bifurcations is the distinction between rotators and vibrators. This distinction was adopted from the case of vanishing electric field strength, so it can be expected to be applicable if the electric field is not too strong. In fact, from figure 12(a) it is obvious that for  $\tilde{E} = -1.4$  and  $\tilde{F} = 0.1$  orbits can uniquely be classified as rotators or vibrators and can be assigned both a series number and a repetition number. However, for long orbits neighboring series of rotators already start to overlap in the plot, and if the electric field strength is increased to  $\tilde{F} = 0.6$ , all orbits get completely mixed up, producing the somewhat messy picture shown in figure 12(b). The relative strengths of the electric and magnetic fields can conveniently be compared if, instead of scaling the magnetic field strength to 1 as described in section II, the scaling properties of the Hamiltonian are used to scale the energy to  $E = -1$ . For the present parameter values, the scaled field strengths are then  $\tilde{B} = 0.60$  and  $\tilde{F} = 0.30$ , so that the magnetic field is still stronger than the electric field, although the latter is no longer negligibly small. Thus, the pattern of orbits should still be dominated by the magnetic field, but figure 12(b) suggests that there is no way to achieve a classification.

A more suitable starting point for a classification is provided by the complete trajectories. Of course, since the classification must gradually break down for sufficiently strong electric fields, it can only be based on heuristic criteria. The criteria we are going to propose are largely based on the behavior of the  $z$ -coordinate of

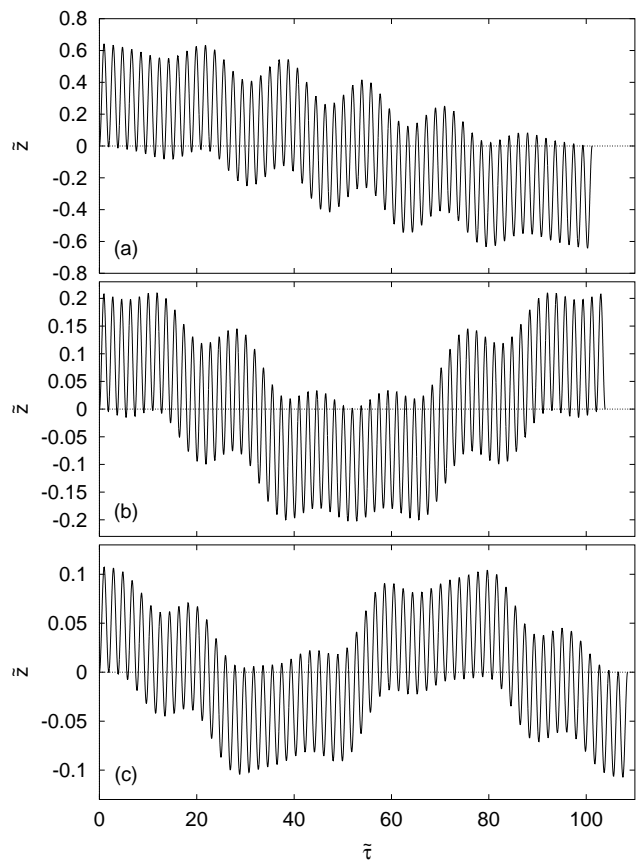


FIG. 21: Rotor orbits of the (a) first, (b) second and (c) third series: scaled coordinate  $\tilde{z}$  as a function of the scaled pseudotime  $\tilde{\tau}$  for  $\tilde{E} = -1.4$  and  $\tilde{F} = 0.2$ .

the motion as a function of time. To illustrate them, this function is plotted for rotators of roughly equal length from different series in figure 21. Figure 22 shows the analogous data for vibrators.

First of all, vibrators are connected to an orbit along the  $z$ -axis in the pure magnetic field case. In this limit, the motion takes place either “above” the  $x$ - $y$ -plane, i.e. in the half-space  $z > 0$ , or “below” the plane. Rotators, on the contrary, stem from the elementary orbit in the plane. Their motion takes place both above or below the plane. Rotators can therefore be distinguished from vibrators if the maximum and minimum values of the coordinate  $z$  are compared: For a rotator, they must have roughly equal absolute values, whereas for a vibrator “above” the plane, the minimum value is much smaller in magnitude than the maximum value.

For the vibrators of a given length shown in figure 22, this criterion gets better the higher the series of the vibrator is chosen. For the vibrator of the first series, which is closest to the domain of rotators, the excursion into the lower half space is of the same order of magnitude as that into the upper half space. As the electric field strength increases further, the vibrator orbit will eventually become indistinguishable, by the present criteria,

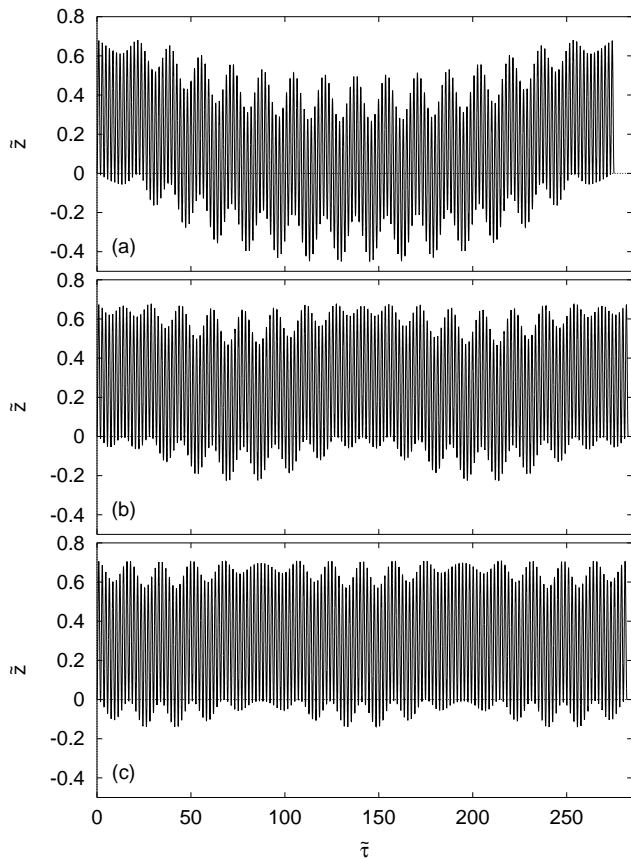


FIG. 22: Vibrator orbits of the (a) first, (b) second and (c) third series: scaled coordinate  $\tilde{z}$  as a function of the scaled pseudotime  $\tilde{\tau}$  for  $\tilde{E} = -1.4$  and  $\tilde{F} = 0.2$ .

from a rotator of the second series.

It has already been noted in the discussion of orbital symmetries that a rotator of the first series that starts from the nucleus into the upper half space returns to it from the lower half space, whereas a rotator of the second series returns from the upper half space. This alternation between motion in the upper and lower half spaces is obvious from figure 21. It can be used to determine the series of a rotator. If the value of  $z(\tau)$  in a maximum is compared to its value in the subsequent minimum, the transitions between motion in the upper and lower half spaces can easily be monitored.

Assigning a series number to a vibrator is considerably more difficult. It relies on the beat structure present in  $z(\tau)$  for a vibrator. Subsequent maxima of this function have varying heights. We consider the maxima that have minimal height compared to neighboring maxima, i.e. the minima of the beats apparent in figure 22. The height of these beat minima slowly oscillates, and the number of their oscillations turns out to give the series number of the vibrator. It can be found by counting the number of minima in the oscillation. Notice that the method uses extrema of the third order: the minima in the minima in the height of maxima. It therefore requires

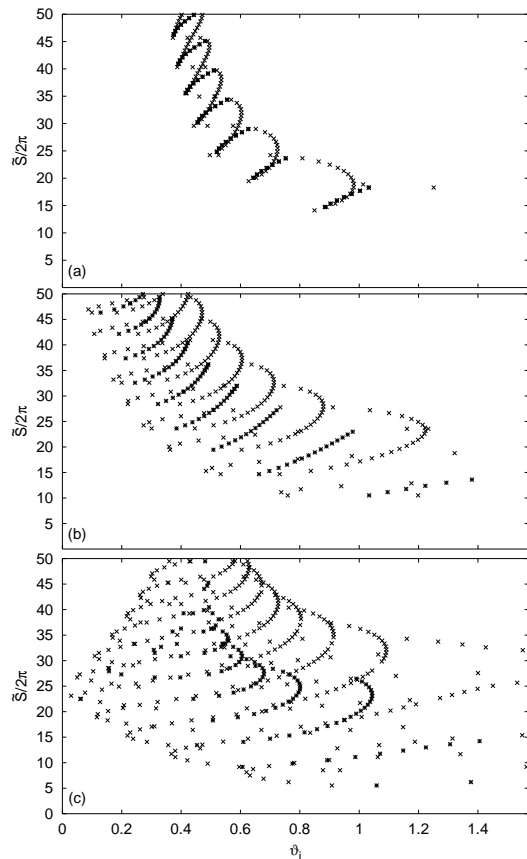


FIG. 23: Rotators of the first series for  $\tilde{E} = -1.4$  and (a)  $\tilde{F} = 0.2$ , (b)  $\tilde{F} = 0.4$ , and (c)  $\tilde{F} = 0.6$ . C-doublets are indicated by  $\times$  symbols, quartets by  $*$  symbols.

vibrators of sufficiently high repetition numbers, so that many maxima of  $z(\tau)$  exist. The method will fail when applied to vibrators of very small repetition numbers. However, these vibrators exist for fairly high scaled energies only, where even in the absence of an electric field the dynamics is mixed or chaotic. In these regions, the classification suggested here might not be meaningful at all.

Finally, orbits can be assigned a repetition number. For vibrators, this can be done by simply counting the number of maxima in  $z(\tau)$ . For rotators, maxima in  $\rho(\tau)$  must be counted, where  $\rho = (x^2 + y^2)^{1/2}$  is the distance from the magnetic field axis. In this case, an additional difficulty arises because  $\rho$  cannot assume negative values, so that between two maxima corresponding to repetitions of the elementary orbits, additional maxima arise from the “swing-by” around the nucleus. These maxima tend to be extremely small and narrow close to the beginning and the end of an orbit, so that they are hard to detect, but they can reach considerable heights in the middle of an orbit. The present form of the classification algorithm, which is certainly open to improvements, counts a maximum in  $\rho(\tau)$  if its height exceeds a certain fraction of the height of the previous maximum. In this form, the

assignment of rotator repetition numbers turns out to be the least robust part of the classification procedure.

The criteria described above readily lend themselves to a numerical implementation, so that the classification of orbits can be achieved automatically. As an example, the rotators of the first series are shown in figure 23 for three different electric field strengths. Although the neat “wiggly-line” structure characterizing the series in figure 11 quickly breaks down for larger electric field strengths, the distinction between different series persists. Figure 23(c) should be compared to figure 12(b). It might appear surprising that the messy-looking set of orbits still permits a classification, but with the help of the criteria just described an ordered pattern of closed orbits can still be discerned. In this sense, the classification scheme derived from the DKP turns out to be remarkably robust.

## VII. SUMMARY

In this work, a systematic study of the closed classical orbits of the hydrogen atom in crossed electric and

magnetic fields has been carried out. As an important step towards a complete understanding of the complicated pattern of closed orbits, a bifurcation theory of closed orbits was developed and the generic bifurcations of codimension one were identified.

A variety of bifurcation scenarios observed in the crossed-fields system was described. They demonstrate that, even though only two types of elementary bifurcations exist, they combine into a wealth of complicated bifurcation scenarios. The abundance of bifurcations exacerbates both a complete classical description of the crossed-fields hydrogen atom and its semiclassical treatment [21].

Based on the classification of closed orbits in the hydrogen atom in a magnetic field, heuristic criteria have been proposed which allow a systematization of closed orbits for moderately high electric field strengths. Although the present analysis cannot yet claim to have achieved a complete classification of closed orbits in the crossed-fields hydrogen atom, it does give a detailed impression of how orbits bifurcate as the electric field strength increases. It thus introduces a high degree of order into the complex set of closed orbits.

- 
- [1] M. L. Du and J. B. Delos, Phys. Rev. A **38**, 1896 and 1913 (1988).
  - [2] E. B. Bogomolny, Sov. Phys. JETP **69**, 275 (1989).
  - [3] J. Main, Ph.D. thesis, Universität Bielefeld, Germany (1991).
  - [4] J. Main, G. Wiebusch, A. Holle, and K. H. Welge, Phys. Rev. Lett. **57**, 2789 (1986).
  - [5] M. A. Al-Laithy, P. F. O’Mahony, and K. T. Taylor, J. Phys. B **19**, L773 (1986).
  - [6] M. A. Al-Laithy and C. M. Farmer, J. Phys. B **20**, L747 (1987).
  - [7] J. Main, A. Holle, G. Wiebusch, and K. H. Welge, Z. Phys. D **6**, 295 (1987).
  - [8] J.-M. Mao and J. B. Delos, Phys. Rev. A **45**, 1746 (1992).
  - [9] G. Raithel, M. Fauth, and H. Walther, Phys. Rev. A **44**, 1898 (1991).
  - [10] G. Raithel, H. Held, L. Marmet, and H. Walther, J. Phys. B **27**, 2849 (1994).
  - [11] J. Rao, D. Delande, and K. T. Taylor, J. Phys. B **34**, L391 (2001).
  - [12] S. Freund, R. Ubert, E. Flöthmann, K. Welge, D. M. Wang, and J. B. Delos, Phys. Rev. A **65**, 053408 (2002).
  - [13] M. J. Gourlay, T. Uzer, and D. Farrelly, Phys. Rev. A **47**, 3113 (1993), erratum 48,2508.
  - [14] E. Flöthmann, J. Main, and K. H. Welge, J. Phys. B **27**, 2821 (1994).
  - [15] J. von Milczewski and T. Uzer, Phys. Rev. E **55**, 6540 (1997).
  - [16] D. A. Sadovskii and B. I. Zhilinskiĭ, Phys. Rev. A **57**, 2867 (1998).
  - [17] N. Berglund and T. Uzer, Found. Phys. **31**, 283 (2001).
  - [18] D. M. Wang and J. B. Delos, Phys. Rev. A **63**, 043409 (2001).
  - [19] M. Kuś, F. Haake, and D. Delande, Phys. Rev. Lett. **71**, 2167 (1993).
  - [20] J. Main and G. Wunner, Phys. Rev. A **55**, 1743 (1997).
  - [21] T. Bartsch, J. Main, and G. Wunner, following paper.
  - [22] K. R. Mayer, Trans. AMS **149**, 95 (1970).
  - [23] P. Kustaanheimo and E. Stiefel, J. Reine Angew. Mathematik **218**, 204 (1965).
  - [24] T. Bartsch, *The hydrogen atom in an electric field and in crossed electric and magnetic fields: Closed-orbit theory and semiclassical quantization*. (Cuvillier, Göttingen, Germany, 2002).
  - [25] T. Bartsch, to be published.
  - [26] H. Goldstein, *Classical Mechanics* (Addison-Wesley Publishing Company, Reading, MA, 1965).
  - [27] D. McDuff and D. Salamon, *Introduction to symplectic topology* (Clarendon Press, Oxford, 1995).
  - [28] T. Poston and I. Stewart, *Catastrophe Theory and its Applications* (Pitman, Boston, 1978).
  - [29] P. T. Saunders, *An introduction to catastrophe theory* (Cambridge University Press, Cambridge, UK, 1980).
  - [30] D. P. L. Castrogiano and S. A. Hayes, *Catastrophe Theory* (Addison-Wesley Publishing Company, Reading, MA, 1993).
  - [31] C. Neumann, R. Ubert, S. Freund, E. Flöthmann, B. Sheehy, K. H. Welge, M. R. Haggerty, and J. B. Delos, Phys. Rev. Lett. **78**, 4705 (1997).